# Network Analysis of the Molecular Layer Interneurons in the Cerebellum

Carolina Lidström

Department of Automatic Control
Lund University
Lund, May 2013

Department of Automatic Control
Lund University
Box 118
SE-221 00 LUND
Sweden

ISSN 0280–5316
ISRN LUTFD2/TFRT--5916--SE


Printed in Sweden by Media-Tryck.
Lund 2013

# Abstract

The cerebellum is important for the control of movements, speech as well as mental activities. In the molecular layer of the cerebellum there exist interneurons which role in the cerebellar neural network is not yet fully understood. In this thesis, these interneurons are simulated by mathematical models in order to investigate their connectivity pattern. Further, the input/output behavior of a delimited part of their neural circuit, with and without a biologically relevant feedback loop, is investigated. The interneurons are simulated by the Leaky integrate and Fire model in combination with the Escape Rate model in Spanne's Simulation Environment.

Connectivity patterns that recreate the behavior of the molecular layer interneurons in vivo are found, motivated by the comparison tools used in this thesis. In these connectivity patterns, five groups of interneurons are connected to each other as one creates the shape of a star. The delimited network with these connectivity patterns are suggestively non-linear. They delay and flip their input in order to create their output, with some affect on the shape of the signal. Most probably, the function of the feedback loop is to control the strength and length in time of the output of the cerebellum.

# Acknowledgements

I would like to thank my supervisor Dr. Henrik Jörntell and his research team for their support during the work of this thesis. I would also like to thank Professor Rolf Johansson, with whom I have had many discussions as well as Anton Spanne for his support with the simulation environment.

# Nomenclature

| | |
|---|---|
| BC | Basket cell |
| EPSP | Excitatory postsynaptic potential |
| GrC | Granule cell |
| IPSP | Inhibitory postsynaptic potential |
| ISI | Inter spike interval |
| MLI | Molecular layer interneuron |
| PC | Purkinje cell |
| PCA | Principle component analysis |
| SC | Stellate cell |

# Contents

# 1

# Introduction

## 1.1 Background

The cerebellum is located in the lower back of the scull, separated from the cerebral hemispheres. It has a fundamental role in processing information drawn from the environment and the motor systems [Purves et al. 2001, p. 14]. It is also involved in the control of mental activities [Ito, 2008] as well as speech [Purves et al. 2001, p. 14]. When it comes to coordination and the planning of movements, the cerebellum is crucial. It is important for the learning of motor tasks and the storage of the information that demands [Purves et al. 2001, p. 18].

The molecular layer of the cerebellum, located in its outermost part, includes the dendritic trees of the Purkinje cells (PCs), the parallel fibers and the molecular layer interneurons (MLIs). These interneurons can be divided into the stellate cells (SCs) and the basket cells (BCs) dependent on how deeply they are located in the molecular layer [Palay and Chan-Palay 1974, p.180]. The Purkinje cells are the sole output cells of the cerebellum while the parallel fibers are an extension of the so called granule cells (GrCs) [Palay and Chan-Palay, 1974].

The functionality of the SCs and BCs are not yet fully known. Improved measurement techniques have made it possible to investigate them further. This is important in order to gain a more solid understanding of the functions and behavior of the cerebellar neural circuit [Jörntell et al., 2010]. In Fig. 1.1 on the following page, the topology of the cerebellar circuit is given. The inhibitory synapses between the MLIs are dashed due to that the pattern of these connections is unknown.

For a more thorough description of the biology and neural circuit of the cerebellum, type of cells present as well as the theory about neuron's electrophysiological behavior see [Purves et al., 2001]. For a description of the cerebellar nerve cells and neural connection paths discussed in this thesis see [Palay and Chan-Palay, 1974]. For the properties and neural connections of the MLIs presently known see [Jörntell et al., 2010], [Abrahamsson et al.,2012 ] and [Jörntell and Ekerot, 2003].

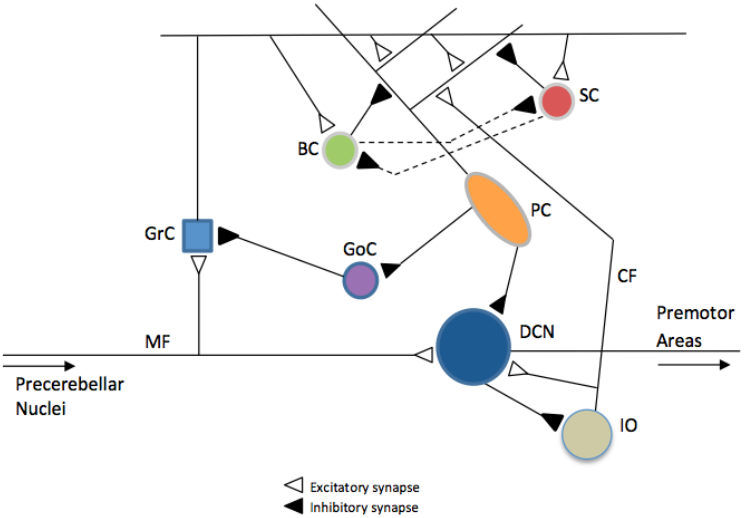


Figure 1.1: Topology of the cerebellar neural circuit, based on [Palay & Chan-Palay, 1974]. MF - Mossy fiber, GrC - Granule cell, SC- Stellate cell, BC - Basket cell, PC - Purkinje cell, GoC - Golgi cell, CF - Climbing fiber, DCN - Deep cerebellar nuclei, IO - Inferior olive.

## 1.2 Statement of the problem

This thesis focuses on the difference in electrophysiological activity between the MLIs and their role in the cerebellar neural network. Their electrophysiological properties will be evaluated as well as the connectivity pattern of their inhibitory synapses. There exists a feedback loop from the PCs back to the GrCs, see Fig. 1.1 above, which will also be investigated. The problem treated in this thesis is stated as follows:

*Investigate different possible network configurations of the MLIs and validate the accuracy of the configuration's behavior by comparison to experimental data. For network configurations with qualitatively the same behavior as found in vivo, investigate their input/output behavior as well their IO-behavior when a feedback loop is present.*

The structure of this thesis is the following; firstly, the methods used are described in the section *Method*. Secondly, a description of the simulations performed is provided for in the section *Simulations* together with a more thorough description in *Appendix A*. Finally, the results and conclusions are given in the last two chapters; *Results* and *Discussion and conclusions*.

## 1.3 Method overview

The experimental data used is provided for at the Department of Medical Sciences, Section for Neurophysiology, Lund University by Henrik Jörntell and his team. The data are in vivo recordings from the cat cerebellum and a full description of how the recordings were made can be found in [Jörntell and Ekerot, 2003]. For a description of the data recorded in GrCs see [Jörntell and Ekerot, 2006] and [Bengtsson and Jörntell, 2009]. In Sec. 2.1 in the following chapter, a brief description of the recordings is given.

The simulation environment used is developed by Anton Spanne at the Department of Medical Sciences, Section for Neurophysiology at Lund University. It is described in [Spanne, 2011]. Signal processing of the experimental and the simulated data is performed in MATLAB, see [MATLAB, 2012], and in-house software is used for extraction of features and sequences of interest in the neural recordings.

# 2

# Method

## 2.1 Characteristics of the MLIs

The experimental data used are presented in Tab. 2.1 below. The data are given numbers which they are referred as henceforth. The behavior of the MLIs are recorded during and after a tactile mechanical stimulation on a skin sensor, stated as the *specific stimulus* in Tab. 2.1.

Measurements of the membrane potentials are sampled every 0.048 ms. The measurements are taken in the cerebellum of a cat which has been decerebrated at the level of the superior colliculus. Bony tentorium has been removed over the recording area, the left cerebellar anterior lobe, to enable recordings with a microelectrode as described in [Ekerot & Jörntell, 2001] and [Jörntell & Ekerot, 2002].

Table 2.1: Experimental data

| # | Cell Types | Description | Nbr of cells and trials |
|---|---|---|---|
| 1 | BC | spike times at two different membrane potentials. | 1 BC, 5 trials at each membrane potential. |
| 2 | SC | spike times after specific stimulus. | 1 SC, 60 trials. |
| 3 | SC and BC | membrane potential during and after specific stimulus. | 6 MLIs at different depth, 10 trials from each cell. |
| 4 | SC and BC | membrane potential during pulse current. | 1 SC and 1 BC, 5 trials from each cell. |
| 5 | GrC | spike times after specific stimulus. | 4 shallow and 4 deep, 15 trials from each cell. |

***Spiking behavior*** The firing activity of a SC, after the specific stimulus, is presented by a histogram of the spike times given in Data 2 in Tab. 2.1. Such a histogram describes the distribution of the spikes, in this case during a 400 ms period after the start of the specific stimulus.

***Membrane potential behavior*** The membrane potentials of the MLIs, during the 100 ms period after the start of the specific stimulus see Data 3 in Tab. 2.1, are analyzed. The trials can be seen as signals and their frequency content and structure are investigated. The mean and trend of the signals are removed by the MATLAB function detrend, motivated by [Gustafsson et al. 2011, p. 84], before they are processed further.

The signals can be described as stochastic time series defined over the entire time axis if truncated by a rectangular window between 0 and approximately 100 ms, resulting in 2048 samples per signal. The Wold's decomposition theorem states, see [Gustafsson et al. 2011, p 92], that every *stationary* stochastic process can be written as the convolution between white noise and some deterministic filter. Therefore, the noise of the signals is analyzed upon if it is white or not.

Dependent on the behavior of the auto-covariance of the signals, estimated by the MATLAB-function covf see [MATLAB, 2012], a suitable time series model is chosen and evaluated, see [Jakobsson, 2011]. Further, the signals are presented in state space by a stochastic realization algorithm, see [Johansson, 2010], as a method of characterization.

The signals have finite energy and their power spectral density is estimated by the fast Fourier transform (FFT) in MATLAB, see fft-function in [MATLAB, 2012] as well as [Gustafsson et al. 2011, p. 52-54]. For a less noisy estimate the Welch's method and the Blackman-Tukey's method can be used, see [Gustafsson et al. 2011, p.105] and [Gustafsson et al. 2011, p.107-110] respectively. In [Pesaran, 2008], a method with multi-tapers for estimation of the spectral density is described. This method is used upon the signals as well. Additionally, the spectral density estimate is derived for sequences of the 100 ms period, as a substitute for wavelet analysis [Bergh et al, 1999].

The variance of the signals is determined for sequences of the entire time period as well. In this case, each sequence comprises one eight of the 100 ms period. Through principle component analysis (PCA), see [Joliffe, 2002], the most important features of the signals are extracted. For this, the MATLAB function pca is used, see [MATLAB, 2012].

## 2.2 Simulation of the MLIs

The connectivity pattern of the MLIs is investigated through simulations by mathematical models of a delimited part of their neural circuit. The simulated behavior is validated against the characteristics of the MLIs found in the experimental data. Further, the network configurations which give rise to realistic behavior of the MLIs are analyzed upon their input/output properties. Finally, the input/output behavior is investigated when a biologically relevant feedback loop is present in the network configurations. The simulations are performed in the simulation environment described in [Spanne, 2011].

## The network structure

The MLIs receive excitatory input from the GrCs while they inhibit each other as well as inhibit the PCs. The neural connections just mentioned are motivated by [Palay and Chan-Palay, 1974]. These connections make up a network, see Fig. 2.1 below. It is this network which is simulated. The uncertainty of the connectivity pattern of the inhibitory synapses among the MLIs is depicted by dashed lines.

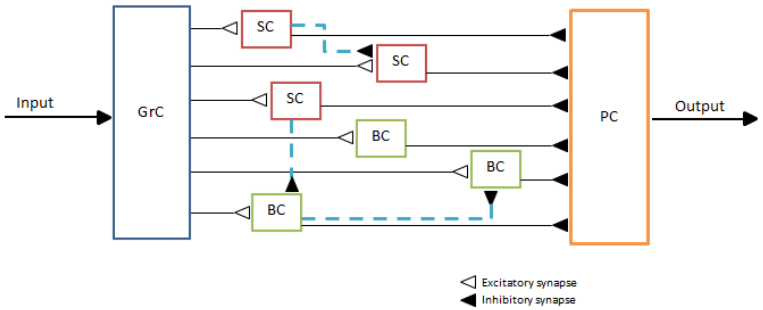


Figure 2.1: Schematic of the network, based on [Palay & Chan-Palay, 1974].

Every MLI receive at least five times as many inhibitory inputs from other MLIs as excitatory inputs from GrCs [Palay and Chan-Palay, 1974; Briatore et al., 2010]. The SCs and the BCs most probably receive GrC-input from both shallowly and deeply located GrCs. There is a possibility that the SCs only receive input from the shallowly located GrCs [Palay and Chan-Palay, 1974].

The BCs are located in the lower third of the molecular layer [Palay and Chan-Palay p.180, 1974] while the SCs make up the outer two thirds [Palay and Chan-Palay p. 216, 1974]. They have similar spiking behavior, a spontaneous firing frequency around 9 Hz [Ruigrok et al., 2011] and a maximum firing frequency of about 500 Hz [Palay and Chan-Palay, 1974]. The cells which the information passes through during the feedback loop are represented by the transfer function $G$, see Fig. 2.2 on the following page.

## The models and their parameters

The behavior of the membrane potential of the SCs and the BCs are modeled by the Leaky Integrate and Fire model, see [Spanne 2011, eq. 2.7] and [Abbott, 1999]. Their spikes are generated by the Escape Rate model, see [Spanne Sec. 3.2, 2011]. This method gives the MLIs a stochastic spiking behavior. Further, the synaptic currents are modeled by the model stated in [Koch & Segev, 1998] and further described in [Spanne 2011, eqs. 2.2-2.4].

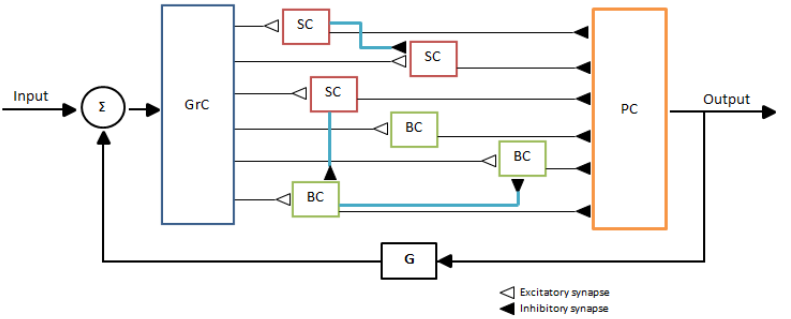


Figure 2.2: Schematic of the network with feedback, based on [Palay & Chan-Palay, 1974].

The models stated have several parameters for which values need to be determined, see *Appendix A* for a description of the model-parameters. For the membrane parameters, two sets of values are used in order to create one model SC and one model BC. They are derived from the shape of the EPSPs given in Data 4, Tab. 2.1, and deemed realistic by comparison to the values stated in [Jörntell & Ekerot, 2003].

The values of the spike parameters of a SC are already determined in [Spanne, 2011] and used in this thesis. The corresponding values for the BC are determined by Data 1 in Tab. 2.1, by the method stated in [Spanne, 2011]. The values of the synapse parameters are determined through optimization of the EPSPs and inhibitory post synaptic potentials (IPSPs) of the simulated SC and BC to such structures shown in vivo, see [Jörntell & Ekerot, 2003].

When the connectivity pattern is investigated, the GrCs are simulated as the spike trains given in Data 5 in Tab. 2.1. Thereafter, they are modeled in the same manner as the MLIs with parameter-values taken from [Jörntell & Ekerot, 2006]. The PC is simulated as a spike to current converter with the membrane parameter-values given in [Jörntell & Ekerot, 2006]. When the network configurations with feedback are simulated, the current from the converter is passed through the transfer function of the feedback loop to then be injected into the GrCs. The simulation setup is described in more detail in *Appendix A*.

# 3

# Simulations

The simulations are executed in three parts; *1. Investigation of the connectivity pattern*, *2. Input/output analysis of the final network configurations* and *3. Input/output analysis of the final network configurations with feedback loop*. The simulation environment has a graphical interface, see Fig 1, 2 and 3 in *Appendix B*. The information obtained, when a neuron is simulated, is the membrane potential and spike times. The sampling time is 0.05 ms.

## 3.1 Part 1. Investigation of the connectivity pattern

The network depicted in Fig. 2.1, if disregarding the PC, is drawn in the simulation environment. Different connectivity patterns of the inhibitory synapses between the MLIs are investigated. The synapse weights of the all the connections present in the network are investigated as well. The behavior of the simulated MLIs are compared to the behavior found in vivo, see Data 2 and 3 in Tab. 2.1.

There are seven different sections of simulations; A, B and 1-5, executed in this order. In section A, the simplest possible connectivity pattern is investigated. That is when all the MLIs present inhibits each other. In each subsequent simulation section the connectivity pattern and synapse weights in the network configurations are altered in order for the simulated behavior to cohere with that seen in vivo. The connectivity patterns and synapse weights investigated in each section are described in *Appendix A* along with comments on the alternations done from one simulation section to the following.

In section 3, two network configurations are able to recreate the behavior of the membrane potential of the MLIs found in vivo, motivated by the comparison techniques used. In order for these systems to recreate the spiking behavior found in vivo, their spiking properties need to be changed. This change is performed in section 5, were the network configurations are given the names *SYS1* and *SYS2*.

## 3.2 Part 2. Input/output analysis of final network configurations

The two final network configurations, SYS1 and SYS2, are analyzed upon their input/output behavior. The GrCs are now simulated by the Leaky Integrate and Fire model with the Escape Rate model for their spike generation, see *Appendix A* for the parameter-values used.

No difference is made between shallowly and deeply located GrCs. In vivo, they are separated due to their input [Bengtsson & Jörntell, 2009]. The input signals used in this analysis do not represent realistic input. Therefore, a distinction between different GrCs-input is not made.

The PC is only investigated upon its membrane potential behavior, see *Appendix A* for parameter-values used for the PC. The input to the network configurations is a bias current while the output is the membrane potential of the PC. The different input currents evaluated are constant, exponential and sinusoidal bias current. This in order to investigate the null-space, zeros and linearity of the configurations.

## 3.3 Part 3. Input/output analysis of final network configurations with feedback loop

The feedback loop is added to the two final network configurations, SYS1 and SYS2, and input/output analysis is performed in the same manner as in part 2. The PC of the feedback loop is modeled as a spike to current converter, with the membrane-parameter-values stated for the PC in Part 2 above.

In the feedback loop, the current from the converter is low-pass filtered, scaled with a gain and delayed in order to simulate the path the information takes back to the GrCs. The parameters of these components are determined by the information given in [Jörntell & Ekerot 2006, Fig. 2], see *Appendix A* for specifics. The input to the network configurations is a bias current while the output is the membrane potential of the PC, as in part 2.

# 4

# Results

## 4.1 Characteristics of the MLIs

Three out of six cells in Data 3 from Tab. 2.1 are useful in this analysis. Remaining data did not show any reaction, in the cells, to the specific stimulus. The three cells are located at different depth in the molecular layer. *Cell 1* is located at a depth of 0.30 mm, *Cell 2* is located at a depth 0.19 mm while *Cell 3* is located at a depth of 0.13 mm. The membrane potential at four stimulation trials of each cell is shown in Fig. 4.1 below. It is *only* the characteristics of these three cells which the simulated MLIs are compared to.

In Fig. 4.2 on the following page, a histogram of 50 spike trains from a SC during the 400 ms period after the start of the specific stimulus is shown. For an equivalent histogram of spike trains from a BC see [Spanne, 2011]. The second *bump* in the histogram in Fig. 4.2 is not due to the specific stimulus but to some other stimulation. This structure is therefore disregarded when the histogram is used for comparison.

The mean and trend of the membrane potentials, hereafter referred to as the signals, are removed. Therefore, they are located around 0 mV instead of -60mV which is the resting potential of the MLIs. If the signals are filtered, for successively

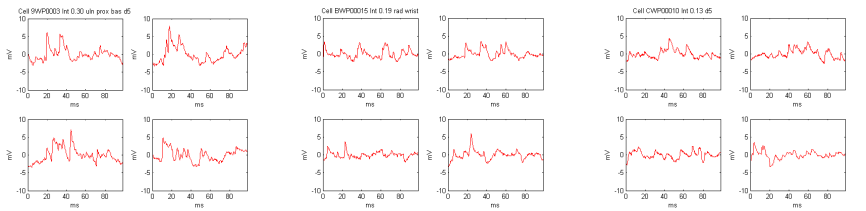

(a) Cell 1: 9WP00003, depth 0.30 mm.

(b) Cell 2: BWP00015, depth 0.19 mm.

(c) Cell 3: CWP00010, depth 0.13 mm.

Figure 4.1: Experimental data: membrane potentials.

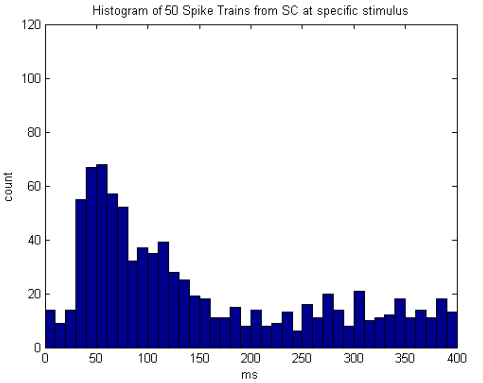


Figure 4.2: Experimental data: Histogram of spike trains after specific stimulus for a SC.

lower cutting frequency of the filter, one notices that the most prominent structure of the signals is represented by frequencies between 100 and 550 Hz.

The auto-covariance of each trial of each cell is shown in Fig. 4.3 on the following page. The subplots represent the different cells. The black line in each graph is the mean value of the auto-covariances shown.

In Tab. 4.1, on the following page, the result of the AR-modeling is given. The tests used to declare the residuals of the models white or not are the sign change test (sc), the cumulative periodogram test (P), the Ljung-Box-Pierce test (LBP), the Monti test (M) and the McLeod-Li test (Ml). These tests are used with a 5% significance level and they are described in [Jakobsson, 2011].

All the signals can be described by AR models. If there is no demand on the model residuals to pass all whiteness tests the order can be kept low. Otherwise, to pass additional whiteness tests the order needs to be higher, see third column in Tab. 4.1. The order of the AR models which are able to represent the signals are spread between 2 and 21. This characterizes the membrane potential signals rather diffusively.

The final-prediction-error test (FPE), see [Jakobsson, 2011, p. 115] , is used to estimate the model orders further. The result of the FPE-test, see last column in Tab. 4.1, states the signals of Cell 1, 2 and 3 as AR processes of order 6, 3 and 2, respectively. This result, of the orders, is still somewhat spread. Therefore, the AR model-approximation is not used in the validation of the simulated signals. Instead, a visual comparison of the auto-covariances is made.

When a stochastic realization algorithm is used, the systems derived are unstable. The signals created by these systems can therefore not be used for comparison with the experimental signals and consequently not be used for the validation of the simulated signals.

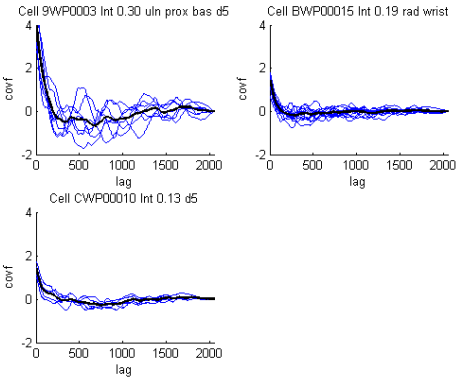


Figure 4.3: Experimental data: Auto-covariance of each trial of each cell. The black lines are the mean of the auto-covariances in each subplot.

Table 4.1: AR approximation

| **Cell** | **Order** | **Cleared WTs** | **FPE** |
|---|---|---|---|
| 9WP00003 | AR(6), all trials except 1 | sc + P | 6 |
| | AR(7) | P | |
| | AR(14), AR(16) | P+LBP+Monti | |
| | AR(16) | P+LBP+Monti | |
| BWP00015 | AR(3), AR(4), AR(5), AR(6) | sc + P | 3 |
| | AR(12), AR(13), AR(14), AR(16) | P+LBP+Mi+ sc | |
| CWP00010 | AR(2) | ML | 2 |
| | AR(3), AR(8) | sc + P | |
| | AR(19), AR(20), AR(21) | P+LBP+M+ sc | |

In Fig. 4.4 on the following page, the spectral density estimate by the multi taper method, for frequencies between 0 and 600 Hz, is shown for the signals of the three cells. The other methods used give the same result. The dashed black lines represent the 95%-confidence intervals of the estimates. The spectral estimate is derived for sequences of the full time length of the signals as well, as a substitute to wavelet analysis. This did not give any new information about the signals.

The variance per time period of the signals from the three cells is given in Fig. 4.5 on the following page. The length of the periods were chosen such that they were able to include one EPSP or IPSP, approximately. The variance is calculated for the respective time period of each signal. The mean of those values for each cell is what is shown in Fig. 4.5. Lines are drawn between the values of the eight time periods.

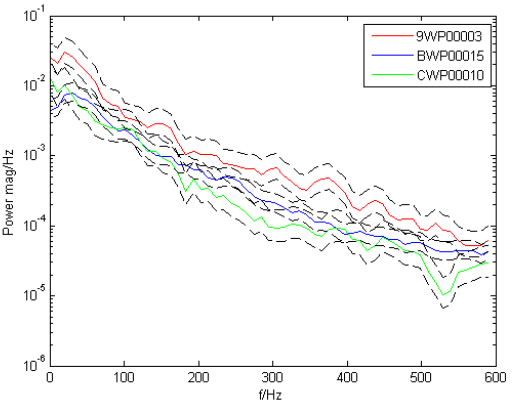


Figure 4.4: Experimental data: Spectral density estimate of the signals of the three cells. Black dotted lines are the 95%-confidence intervals.

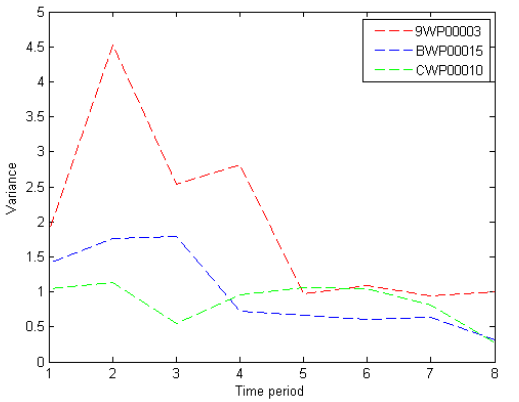


Figure 4.5: Experimental data: The variance in time period 1-8 for the three cells.

The least important components of the signals of each cell, derived by PCA, are stated non white by the whiteness tests used in the AR-approximation described before. PCA upon four signals from each cell results in the principle components pca1 to pca4 given in Fig. 4.6 on the following page. The variance of the components is stated in the titles of the subplots.

Cointegration and wavelet analysis, see [Engle & Granger, 1987] and [Bergh et al., 1999] respectively, are used but do not give any new information about the signals. When the simulated behavior is compared with the behavior found in experiments, a visual comparison of the membrane potentials is made. If there exists

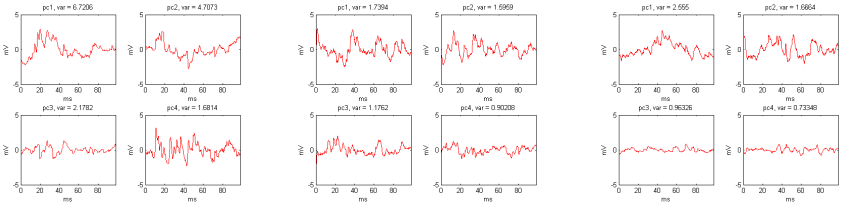


(a) 4 first principal components of cell 1: 9WP00003

(b) 4 first principal components of cell 2: BWP00015

(c) 4 first principal components of cell 3: CWP00010

Figure 4.6: Experimental data: PCA of the membrane potentials.

similarities, the rest of the comparison tools are used for further evaluation. These are the auto covariance, spectral density estimate, variance per time period, principle components as well as the spike train histograms, see Figs. 4.3, 4.4, 4.5, 4.6 and 4.2 respectively.

## 4.2 Simulation of the MLIs

### Part 1. Investigation of the connectivity pattern

Network configurations SYS1 and SYS2 in SIMULATION 5, see *Appendix A*, give rise to realistic behavior for the simulated MLIs. This is motivated by the comparison tools used. The comparison and validation done for the network configurations presented in SIMULATION A, B and 1-4 are reported in *Appendix A*. Their validation failed on some point which deemed them unrealistic.

For comments on the evolution of the simulations and pictures of SYS1 and SYS2 see *Appendix A* and *B*, respectively. The SCs of the two network configurations are identical in their parameter-values and connections while the BCs differ.

The membrane potentials of one of the simulated SCs and one of the BCs of SYS1 and SYS2, during the 100 ms period after the start of the stimulation, are shown in Fig. 4.7 on the following page. Large IPSPs are present in the simulated membrane potentials. This is a behavior which is found in experiments as well, compare Figs. 4.1 and 4.7. The BCs in SYS1 exerts the highest EPSPs and could be coupled with Cell 1 of the experimental data. The SC exerts more damped behavior than the BCs. This is the case for the experimental data as well, compare Cell 1 to Cell 3 in Fig. 4.7. The first 10 ms of each simulated trial shown in Fig. 4.7 include nonrealistic behavior. In the following investigation of the simulated signals, these first 10 ms are therefore disregarded.

In Fig. 4.8 on the following page, 50 spike trains from the start of the specific stimulus and 400 ms ahead are shown for the three simulated cells shown in Fig. 4.7. When compared to the behavior found in experiments, see Fig. 4.2, the peak in the histograms match in both the starting point, length in time, height and shape. In

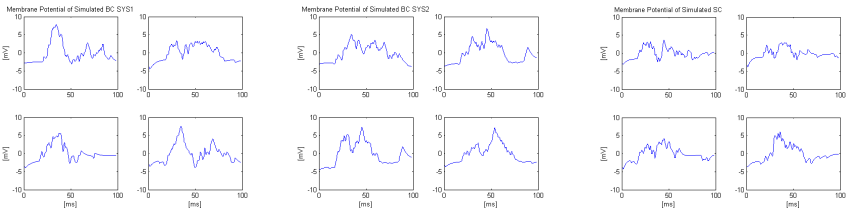


(a) Simulated response from BC in SYS2.

(b) Simulated response from BC in SYS2.

(c) Simulated response from SC in SYS1 and SYS2.

Figure 4.7: Simulated data: membrane potentials.

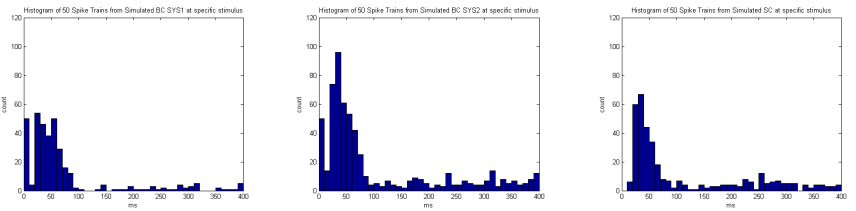


(a) Simulated spike trains from BC in SYS1.

(b) Simulated spike trains from BC in SYS2.

(c) Simulated spike trains from SC in SYS1 and SYS2.

Figure 4.8: Simulated data: Histogram of spike trains after specific stimulus for the simulated SC and BCs.

the simulation of the BCs in SYS1 and SYS2 there often occur a spike during the first 10 ms, something which is not seen in the experimental data.

The mean and trend is removed from the membrane potentials, or signals, presented in Fig. 4.7 before further analysis. By simply filtering with a low-pass filter one notices that the most prominent structure of the signals is given for frequencies between 100Hz and 550Hz, as for the experimental data. The mean of the autocovariances of the signals of the SC and BCs of SYS1 and SYS2 is given in Fig. 4.9 on the following page. The simulated signals seem to be of approximately the same order as the experimental signals, motivated by visual comparison of Fig. 4.9 to Fig. 4.3.

The spectral density estimate of the signals are shown in Fig. 4.10 on the following page. These spectral estimates are similar to the spectral estimates of the experimental data in Fig. 4.4. The BCs have somewhat higher energy for lower frequencies.

The variance of the signals in time period 1-8 is determined in the same manner as for the experimental data. Due to that the first time period of the simulated signals show unrealistic behavior, this period is disregarded. If the time periods of the

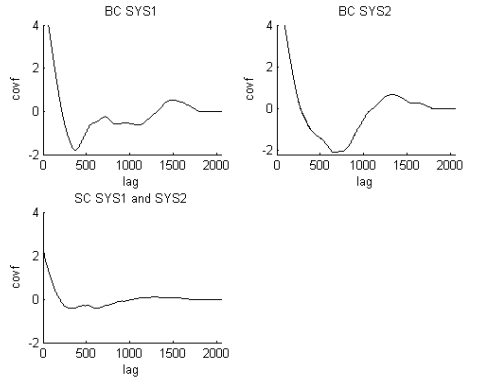


Figure 4.9: Simulated data: Mean of the auto-covariance of the signals of the simulated SC and BCs.

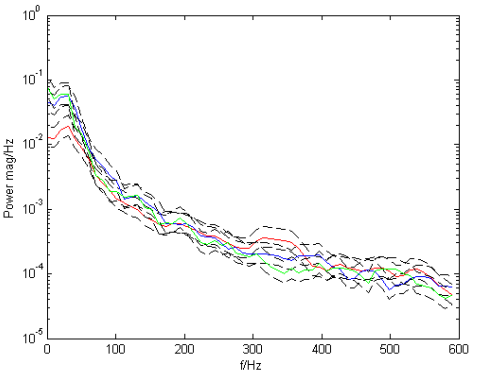


Figure 4.10: Simulated data: Spectral estimate for the signals of each network. Red - SC, Blue - BC SYS1, Green - BC SYS2. The black dotted lines are the 95% confidence intervals.

simulated data are shifted backwards, such that period 2 is seen as period 1 instead, the variance of the simulated signals match the variance of the experimental signals, see Fig. 4.11 on the following page. Otherwise, the response in the simulations is delayed compared to the experimental data. The SC has the lowest variance, while the BC of SYS1 has the highest. The difference in variance between the SC and the BC coheres with what is seen in the experimental data.

The least important components of the simulated signals, derived by PCA, were stated non white as for the experimental signals. PCA was made upon four signals from the SC and the BCs, respectively. This resulted in the principle components

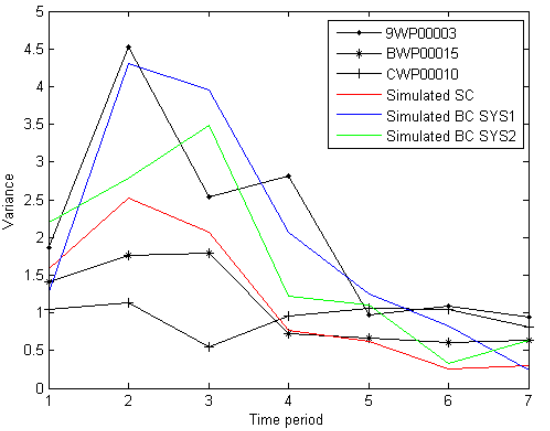


Figure 4.11: The variance in time period 1-7 for the simulated SC and BCs, the variance is shifted one period. The balck lines are the variance of the experimental data.

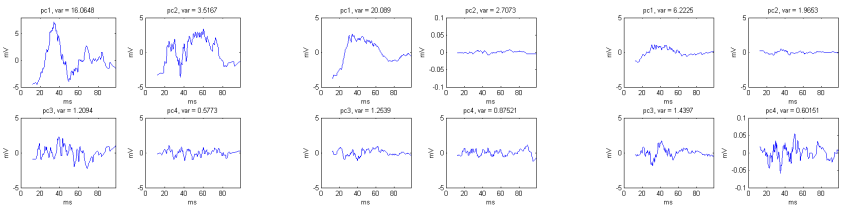

(a) Principal components of BC SYS1

(b) Principal components of BC SYS2

(c) Principal components SC SYS1 and SYS2

Figure 4.12: Simulated data: PCA of the membrane potentials.

pca1 to pca4 given in Fig. 4.12 above. The variances of the components are stated in the titles of the subplots. The simulated SC and BCs all have a first component with higher variance than the first components of the experimental data, see Fig. 4.6. The other components are more similar between the simulated and experimental signals.

## Part 2. Input/output analysis of final network configurations

If the network configurations, SYS1 and SYS2, are given no input they just experience spontaneous activity. This activity affects the PC and lowers its membrane potential. This state of the PC is seen as its ground state. Negative bias currents of any size keeps the PC in its ground state and does therefore not result in any output.

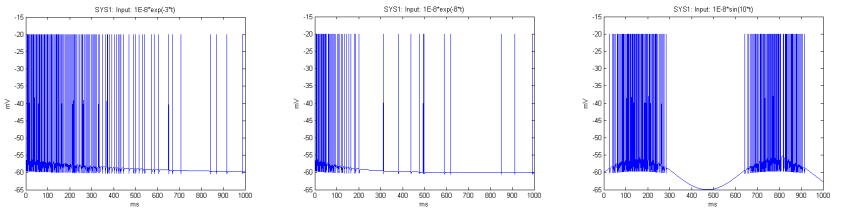

(a) SYS1, Input: 1E-8exp(-3t) A. Shows GrC membrane potential.
(b) SYS1, Input: 1E-8exp(-8t) A. Shows GrC membrane potential.
(c) SYS1, Input: 1E-8sin(10t) A. Shows GrC membrane potential.

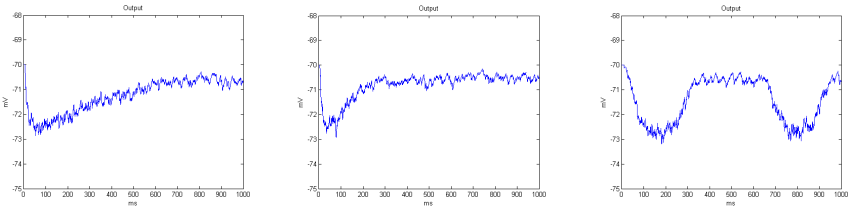

(d) SYS1, Input: 1E-8exp(-3t) A. Shows PC membrane potential.
(e) SYS1, Input: 1E-8exp(-8t) A. Shows PC membrane potential.
(f) SYS1, Input: 1E-8sin(10t) A. Shows PC membrane potential.

Figure 4.13: Input/Output analysis SYS1.

Sinusoidal input signals are shifted 180 degrees and delayed about 5 ms in both SYS1 and SYS2. The delay is present for all input signals. The sinusoidal shape is somewhat affected which suggests that the systems are non-linear. See Fig. 4.13(f) and 4.14(f) for the membrane potential of the PC, the output of the network, at sinusoidal input to SYS1 and SYS2, respectively. In subplot (c) in both figures, the membrane potential of a GrC is depicted in order to show the first impact this input-current has upon the systems.

No system-zeros are found when an exponential function is used as input. Both SYS1 and SYS2 seem to flip the input and delay it to create the output. In Fig. 4.13(d) and 4.13(e), the output of SYS1 at two different exponential currents are shown. The corresponding plots for SYS2 are shown in 4.14(d) and 4.14(e). Subplots (a) and (b) in both figures show the membrane potential of a GrC at the inputs just stated.

When a bias current of 1E-7 A, which is a very high bias current, is inserted to the GrCs in SYS1 the groups of BCs start to synchronize. This behavior is already visible at a bias current of 1E-8 A. The behavior of BCs from two different groups are shown in Fig. 4.15 on the following page. There is a delay between the bursts of the two groups.

No interesting behavior is found for the SCs in SYS1. When inserting the same type of bias current to the GrCs in SYS2 the BCs experience a very high firing

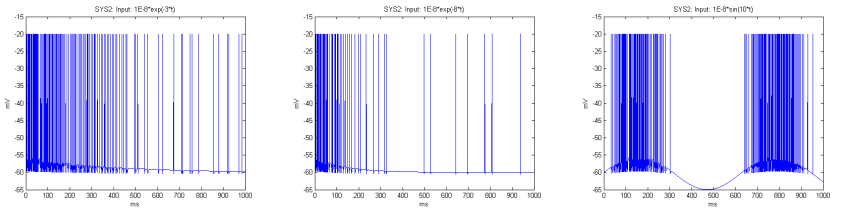

(a) SYS2, Input: 1E-8exp(-3t) A. Shows GrC membrane potential.

(b) SYS2, Input: 1E-8exp(-8t) A. Shows GrC membrane potential.

(c) SYS2, Input: 1E-8sin(10t) A. Shows GrC membrane potential.

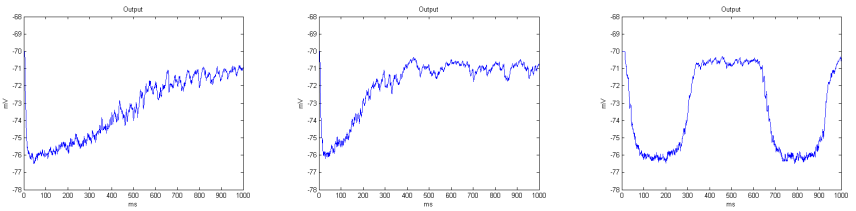

(d) SYS2, Input: 1E-8exp(-3t) A. Shows PC membrane potential.

(e) SYS2, Input: 1E-8exp(-8t) A. Shows PC membrane potential.

(f) SYS2, Input: 1E-8sin(10t) A. Shows PC membrane potential.

Figure 4.14: Input/Output analysis SYS2.

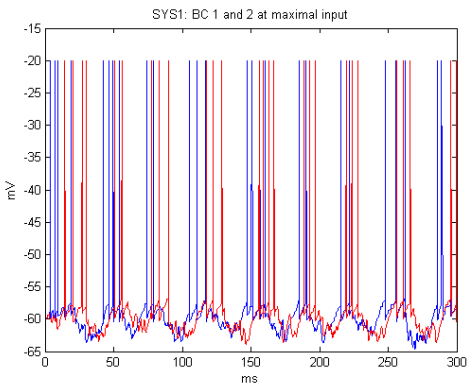


Figure 4.15: Membrane potential of BCs from two different groups in SYS1.

frequency, about 200 Hz. The SCs are not showing any extraordinary behavior.

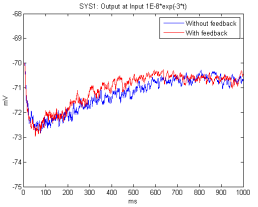


(a) SYS1 with feedback, Input: 1E-8exp(-3t) A. Shows PC membrane potential.

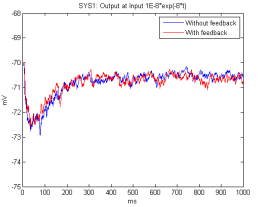


(b) SYS1 with feedback, Input: 1E-8exp(-8t) A. Shows PC membrane potential.

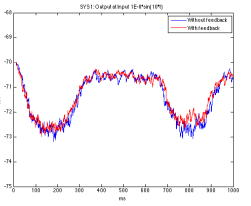


(c) SYS1 with feedback, Input: 1E-8sin(10t) A. Shows PC membrane potential.

Figure 4.16: Input/Output analysis SYS1 with feedback

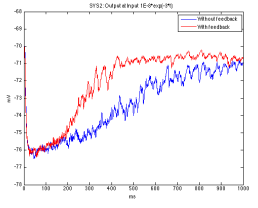


(a) SYS2 with feedback, Input: 1E-8exp(-3t) A. Shows PC membrane potential.

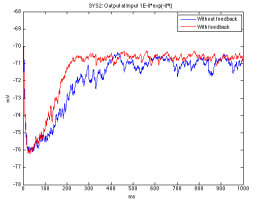


(b) SYS2 with feedback, Input: 1E-8exp(-8t) A. Shows PC membrane potential.

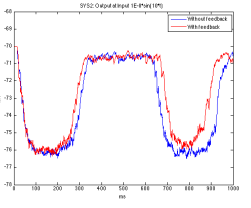


(c) SYS2 with feedback, Input: 1E-8sin(10t) A. Shows PC membrane potential.

Figure 4.17: Input/Output analysis SYS2 with feedback

## Part 3. Input/output analysis of final network configurations with feedback loop

The input signals used in Part 2 are used in this third part of the simulations as well. The low-pass filter used in the feedback loop has a cut-off frequency of 10 Hz, the gain is 0.2 and the delay is 10 ms, see *Appendix A* on how these values are derived.

None or negative bias current gives no output from the network configurations with feedback. In Fig. 4.16 above, the outputs of SYS1 with as well as without feedback are given. Corresponding graphs for SYS2 are given in Fig. 4.17 above. The feedback loop seems to shorten the output of the network, make it more distinct in the time domain as well as decrease its strength. In subfigure (c) of both Fig. 4.16 and 4.17 it is clear that the feedback loop dampens the output of the systems. The outputs still experience a delay of about 5 ms.

At high input bias currents it seems as if the SCs of SYS1 with feedback start to synchronize as well, additional to the BCs. The BCs of SYS2 still react to high input bias currents with a high firing frequency.

# 5

# Discussion and conclusions

Different connectivity patterns have been investigated in order to get closer to an answer on how the connections between the MLIs are organized. Two of the simulated network configurations result in MLIs that behave as in vivo, motivated by the comparison tools used in this thesis. This indicates that the connectivity pattern and synapse weights used in these two network configurations, with names SYS1 and SYS2, most probably can be found in reality. The input/output of the configurations, with and without a biologically relevant feedback loop, is identified.

Alongside with the simulations, additions has been made to the simulation environment by its developer on the request of the author of this thesis.

## 5.1 About the results

### Comparison technique

The membrane potentials of the MLIs, given in the experimental data during the 100 ms period after the start of the specific stimulus, have rather vague characteristics. Their main frequency domain is between 100 and 550 Hz and they can be approximated as AR models of second or higher order. Further, their variance during the 100 ms period can take on values between 0.4 and 4.5 in some recurrent structure. This vagueness makes it more difficult to evaluate if the simulated behavior is realistic or not.

The most successful comparison techniques are visual comparison of the membrane potential, the spike trains and the variance. When the Stochastic Realization algorithm is used, the systems derived are found unstable. This is a result which is not completely obvious. This method as well as the AR-approximation method should be evaluated further.

The major limitation of the validation-process is the lack of sufficient experimental data. There is also a need for development of a better comparison tool. In the mean time, comparison of the auto covariance, spectral density estimate as well as the principle components can be used.

## Simulation setup

When the simulation environment is used, it is possible to analyze the behavior of a large set of neurons at the same time. This is something which is still difficult to do in in vivo and in vitro studies. When a large set of neurons is simulated, it is crucial to use rather simple models in order to achieve a short compilation-time. Of course, this limits the order of detail in in the simulations. The combination of mathematical detail in the models and number of neurons simulated which give the most accurate result without being too computationally demanding must be pursued.

The large IPSPs observed in the simulated membrane potentials of the MLIs in SYS1 and SYS2 are due the synchronization of spikes between interneurons. This is a behavior which is present in vivo as well. Considering the fact that the network configurations are able to recreate this phenomenon, the models and simulation setup used seem detailed enough. The phenomenon of the large IPSPs started to occur when the *star-shape* connectivity pattern was used, see *Appendix A* for description.

The Escape Rate model, for simulation of the stochastic behavior of the spike generation in the neurons, is both validated and invalidated in [Dürango, 2010]. Therefore, this method needs to be evaluated more thoroughly in order to investigate the impact it has on the simulations and how valid it is. The Escape Rate model describes the times of subsequent spikes as a point process which states the spike-times independent of each other. In reality, they might be inter-dependent as discussed in [Ekholm & Hyvärinen, 1970]. Again, a benefit of the Escape Rate model is that it takes into account the refractory period, the minimum time observed between two subsequent spikes in vivo.

The synaptic activity of a neuron is in fact highly stochastic which it is not modeled as in the simulations done in this thesis. Some stochastic representation could be needed in order to simulate the network correctly. On the other hand, it might be compensated by the other stochastic behavior simulated, motivated by [Hillie, 2001].

## Simulation results

The first 10 ms of the simulated membrane potentials does not show realistic behavior. Neither does the spiking activity during this period, especially for the simulated BCs. This is most probably due to that the simulated MLIs receive no input until the first time the GrCs spike, due to the stimulation. This is not the case in vivo, where the MLIs receive input from other paths in the neural network in addition to the stimulation path. The behavior created by the additional input is present in the experimental data but it is not simulated. When the alternation in the simulated membrane potentials is slow, it is more likely for the Escape Rate model to initiate a spike.

The simulated BCs have somewhat higher energy for lower frequencies than the BCs in experiments. The auto-covariances of the simulated signals vary more

than the auto-covariances of the experimental signals and all simulated cells have a first principle component of higher variance than the cells in experiments do. These differences are most probably also an outcome of that it is just a restricted part of the entire neural network which is simulated.

In Fig. 4.11, the variance of the simulated membrane potentials is shifted one time period backwards. It is more likely the variance of the experimental data which should be shifted forward in time instead. In Fig. 4.2, one can see that the response from the stimulus does not start until 20 ms after the stimulation onset, which is equivalent with time period 2. This is the case for the simulated cells in Fig. 4.8 as well. When the membrane potential in the experimental data has been extracted, the stimulation onset must have been determined wrongly.

The network configurations without feedback flip and delay their input signal in order to create their output, with some affect on the shape of the signal. The delay is most likely linked to the time it takes for the input current to make the GrCs spike for the first time in each trial.

The feedback loop regulates the output of the network configurations such that it decreases its strength and makes it last shorter in time. When something changes in the cerebellar circuit, the feedback loop's role is most probably to control the output of the cerebellum by keeping it in a certain interval, both in size in mV and length in time. Of course, the feedback loop controls the activity of the GrCs as well which coheres with the findings presented in [D'Angelo, 2008].

The values of the spike parameters used in SIMULATION A,B and 1-4 had to be changed in SIMULATION 5 because they resulted in unrealistic behavior. The values used in the first six simulation sections were based on experimental data. When the membrane potential of a cell is measured, an access resistance is created because of the measuring equipment. This makes it hard to determine the membrane potential exactly which of course give false information and consequently false values for the spike parameters.

The membrane potentials and spike trains that arise from the specific stimulus can be described as the response to natural touch or stretch of the skin. The GrCs can be divided into groups which are responsible for the input from different specific locations on the skin. Therefore, if the skin of the back of a hand is stretched the behavior shown in this thesis will be the case for the MLIs that receive input from the GrCs responsible for that specific area.

Further, the membrane potential signals of the experimental data can be described by AR models of order 2, 3 and 6. This states dynamical systems with various complexity. All membrane-potential-signals, both experimental and simulated, can be seen as the potential in an electrical circuit with a capacitance and a conductance in parallel, as modeled by the Leaky Integrate and Fire model [Abbott, 1999].

## 5.2 Future work

The models and parameters used for the different neurons need to be validated by a larger set of experimental data which includes responses to other types of stimuli as well. Additional network configurations need to be tested and the simulation implementation needs to be done according to statistical design of experiments. More than one model SC and BC need to be used in order to cover a larger scope of the MLIs that exist in reality.

The final network configurations should be expanded to include a larger functional circuit of the neural network. It is often easier to evaluate the behavior of larger networks due to that they have been more closely examined. The larger networks can be evaluated upon if they are able to predict in vivo behavior.

Hopefully, additional experimental data will give a more distinct picture of the characteristics of the MLIs. This would make the validation of the simulated connectivity patterns easier. Betters tools for comparison need to be investigated as well. The simulation environment needs improvements such as making it easier to simulate larger sets of neurons.

There is much that need to be answered about the functionality and the role of the molecular layer interneurons in the cerebellum. It is a research field which is crucial in order to be able to fully understand the neural network and in particular the cerebellar neural network.

# Appendix A

This is a description of the simulations performed in the work of this thesis. The simulations can be divided into seven different sections. The different network configurations, therein connectivity patterns, of each simulation section are given names. After each network description, a summary of the amount of excitatory and inhibitory input is given in italic. Before the network configurations of each section are described, a short description of the major simulation properties are given.

## Part 1: Investigation of the connectivity pattern

### SIMULATION A

The values of the membrane, synapse and spike parameters presented in Tab. 1, 2 and 3 below are used in this simulation section. The values of the spike parameters are derived in [Spanne, 2011]. They are used both for the model SC and the model BC due due to that Data 1 in Tab. 2.1, Chap. 2, Sec. 2.1, resulted in non-realistic properties for the BC spiking behavior. To have the same spike parameters for the model SC and the model BC is motivated by [Jörntell et al., 2010] which states that the functions of the two types of interneurons most probably are alike.

The membrane parameters are the membrane time constant $\tau$, the resistance $R_m$, capacitance $C_m$, conductance $g_L$ as well as resting potential $E$. The hyper polarization value $V$ and ion conductance $K$ are set to 0.5 and 8, respectively. They do not have that great of an impact unless the spiking intensity is really high, which is not the case for the simulations in this thesis. The membrane and synapse parameter values are derived from Data 4 in Tab. 2.1.

#### SC simulation

**S1AA:** Network of 10 SCs, every SC inhibits the other SCs three times. A SC has input from 4 shallow GrCs, totally 9 shallow GrCs present. Close SCs share some input from the same GrCs, but never from a completely identical set.

*4 excitatory and 27 inhibitory inputs (every third synapse is from the same cell).*

Table 1: Values of the membrane parameters

| Parameter | SC | BC |
|---|---|---|
| $\tau$ (ms) | 2 | 4 |
| $R_m$ (MΩ) | 125 | 125 |
| $C_m = \tau / R_m$ (F) | 1.6E-11 | 3.2E-11 |
| $g_L = 1/R_m$ (S) | 8E-9 | 8E-9 |
| $E$ (mV) | -60 | -60 |
| $V$ (mV) | -0.5 | -0.5 |
| $K$ | 8 | 8 |

Table 2: Values of the synapse parameters

| Parameter | Excitatory | Inhibitory |
|---|---|---|
| *Delay* (ms) | 5E-4 | 5E-4 |
| $\alpha$ | 3.7E-4 | 5.4E-4 |
| $\beta$ | 5.4E-4 | 6.5E-4 |
| $T_{max}$ | 0.0 | 0.0 |
| *td* | 5.4E-4 | 6.2E-4 |
| $E$ (mV) | 0 | -80 |
| *Weight* | 1E-9 | 1E-9 |

Table 3: Values of the spike parameters

| Parameter | Values |
|---|---|
| ISI mean | [2,11883,-30,4] |
| ISI std intensity | [10243,-10245,-23,-4.7] |

**S3AAB:** As S1AA but each SC receives 10 extra inhibitory inputs, one from every BC in B1AA, see description below.

*4 excitatory and 37 inhibitory inputs (10 of which are from BCs).*

**S4AABZ:** As S3AAB but the SCs inhibit the BCs as well, in the same manner. This is the same network as B4AASZ.

*4 excitatory and 37 inhibitory inputs (10 of which are from BCs).*

**S5AAC:** As S1AA but the value of the conductance is 2.3E-11 instead.

*4 excitatory and 27 inhibitory inputs.*

**S6CL:** Network of 15 SCs, every SC inhibits its 8 closest neighbors (close if they share GrC-input) 3 times. A SC has input from 4 shallow GrCs, totally 16 shallow GrCs present. Close SCs share some input from the same GrCs, but never from a completely identical set.

*4 excitatory and 24 inhibitory inputs.*

## BC simulation

**B1AA:** Network of 10 BCs, every BC inhibits the other BCs three times. A BC has input from 4 deep GrCs, totally 9 deep GrCs present. Close BCs share some input from the same GrCs, but never from a completely identical set.

*4 excitatory and 27 inhibitory inputs.*

**B2AA:** Network of 17 BCs, every BC inhibits the other BCs two times. A BC has input from 4 deep GrCs, totally 12 deep GrCs present. Close BCs share some input from the same GrCs, but never from a completely identical set.

*4 excitatory and 32 inhibitory inputs.*

**B3AAS:** As B1AA but each BC receives 10 extra inhibitory inputs, one from every SC in S1AA.

*4 excitatory and 37 inhibitory inputs (10 of which are from SCs).*

**B4AASZ:** As B3AAS but the BCs inhibits the SCs as well, in the same manner. This is the same network as S4AABZ.

*4 excitatory and 37 inhibitory inputs (10 of which are from SCs).*

**B5AAC:** As B1AA but the value of the conductance is 2.3E-11 instead.

*4 excitatory and 27 inhibitory inputs.*

**B6CL:** Network of 15 BCs, every BC inhibits its 8 closest neighbors (close if they share GrC-input) 3 times. A BC has input from 4 shallow GrCs, totally 16 shallow GrCs present. Close BCs share some input from the same GrCs, but never from a completely identical set.

*4 excitatory and 24 inhibitory inputs.*

**B7SH:** As B1AA but one fourth of the GrC-input to the BCs comes from shallow GrCs instead of deep. These measurements are from a BC with no direct input from shallow GrCs.

*4 excitatory and 27 inhibitory inputs.*

**B8SHD:** As B7SH but these measurement are from a BC with direct input from shallow GrCs, 2/4 synapses.

*4 excitatory and 27 inhibitory inputs.*

**Conclusions from SIMULATION A:**
It is not reasonable that the membrane resistance and time constant for the SCs and BCs are identical, motivated by the values determined in [Jörntell & Ekerot, 2003]. Therefore, these values are changed in the following simulations to values given in [Jörntell & Ekerot, 2003], see Tab. 4 below. The synapse-parameter-values stated in Tab. 2 are changed as well. This in order for the simulated cell's EPSPs and IPSPs to fit such structures found in experiments, see [Jörntell & Ekerot, 2003].

Simulated trials of the SCs and BCs in the different network configurations are evaluated by comparison to in vivo behavior. Firstly, a visual comparison of the membrane potential, during the 100 ms period after the start of the specific stimulus, is performed. Network S1AA and S6CL look similar to the experimental data except from some very large IPSPs. This behavior is due to the network setup, where one SC is able to inhibit another SC with synapse weight 3. In order to make the inhibitory input to each MLIs more diverse, the number of SCs and BCs is increased to 25 in the following simulations. The remaining network configurations do not share any characteristics with the experimental data.

## SIMULATION B

The values of the membrane parameters used in this simulation section are stated in Tab. 4 below while the values of the synapse parameters are stated in Tab. 5 on the following page. Further, the value of the spike parameters used are given in Tab. 3 on page 26. This set of values of the model-parameters are used in SIMULATION 1-4 as well. The weight of each synapse is a simulation parameter and therefore not stated in Tab. 5 but in each network configuration instead.

Table 4: Values of the membrane parameters

| Parameter | SC | BC |
|---|---|---|
| $\tau$ (ms) | 3 | 6 |
| $R_m$ (MΩ) | 200 | 100 |
| $C_m = \tau / R_m$ (F) | 1.5E-11 | 6E-11 |
| $g_L = 1/R_m$ (S) | 5E-9 | 1E-8 |
| $E$ (mV) | 60 | 60 |
| $V$ (mV) | 0.5 | 0.5 |
| $K$ | 8 | 8 |

**SC simulation**
Receives only shallow GrC
Synapse weight inhibitory: 1E-9.
Synapse weight excitatory: 1E-9.

Table 5: Values of the synapse parameters

| Parameter | Excitatory | Inhibitory |
|---|---|---|
| *Delay* (ms) | 5E-4 | 5E-4 |
| $\alpha$ | 2E-4 | 2E-4 |
| $\beta$ | 3E-4 | 3E-4 |
| $T_{max}$ | 0.0 | 0.0 |
| *td* | 3E-4 | 3E-4 |
| *E* (mV) | 0 | -75 |
| *Weight* | - | - |

**S1AA:** Network of 25 SCs, every SC inhibits all other SCs once. One SC receives input from 4 shallow GrCs, totally 10 shallow GrCs present. Close SCs share some input from the same GrCs, but never from a completely identical set.

*4 excitatory and 24 inhibitory inputs.*

**S2AAB:** As S1AA but close SCs (close means that they share the somewhat the same GrC-input) receive inhibitory input from 6 close BCs in B1AA, se description below.

*4 excitatory and 30 inhibitory inputs (6 of which are from BCs).*

**S4AABZ:** As S2AAB but the SCs inhibit the BCs as well, in the same manner. This is the same network as B4AASZ, see below.

*4 excitatory and 30 inhibitory inputs (6 of which are from BCs).*

**S4AABZshall:** As S4AABZ but the BCs receive some input from shallow GrCs. 30/100 excitatory synapses are from shallow GrCs.

*4 excitatory and 30 inhibitory inputs (6 of which are from BCs).*

**S6CL:** As S1AA but ten close SCs has twice the synapse weight among each other. The membrane potential of one of these cells is of interest.

*4 excitatory and* 24 *inhibitory inputs (higher synapse weight for some, see specificity above).*

## BC simulation

Receives only deep GrC

Synapse weight inhibitory: 1E-9.

Synapse weight excitatory: 1E-9.

**B1AA:** Network of 25 BCs, every BC inhibits all other BCs once. One BC receives input from 4 deep GrCs, totally 10 deep GrCs present. Close BCs share some input

from the same GrCs, but never from a completely identical set.

*4 excitatory and 24 inhibitory inputs.*

**B2AAS:** As B1AA but close BCs receive inhibitory input from 6 close SCs in S1AA.

*4 excitatory and 30 inhibitory inputs (6 of which are from SCs).*

**B4AASZ:** As B2AAS but the BCs inhibit the SCs as well, in the same manner. This is the same network as S4AABZ.

*4 excitatory and 30 inhibitory inputs (6 of which are from SCs).*

**B4AASZshall:** As B4AASZ but 30/100 excitatory inputs to the BCs are from shallow GrCs.

*4 excitatory and 30 inhibitory inputs (6 of which are from SCs).*

**B6CL:** As B1AA but ten close BCs has twice the synapse weight among each other. The membrane potential of one of these cells is of interest.

*4 excitatory and* 24 *inhibitory inputs (higher synapse weight for some, see specificity above).*

**B7AAshall:** As B1AA but 30/100 inputs come from shallow GrCs.

*4 excitatory and 24 inhibitory inputs.*

### Conclusions from SIMULATION B:

In this simulation section, all BC-network-configurations show very low variance behavior for the membrane potentials of the BCs. This is not the case in the experimental data. Therefore, their synapse weights are increased in the following simulation sections. The following simulation section, SIMULATION 1, includes some of the networks configurations given in this simulation section but the BCs have higher synapse weights. The evaluation of the SCs is done in that simulation section instead. SIMULATION 2 is identical to SIMULATION 1, apart from that the SCs and BCs receive input from both shallowly and deeply located GrCs in SIMULATION 2.

## SIMULATION 1

### SC simulation

Receives only shallow GrC input.

Synapse weight inhibitory: 1E-9.

Synapse weight excitatory: 1E-9.

**S1AA:** Network of 25 SCs, every SC inhibits all the other SCs once. One SC receives input from 4 shallow GrCs, totally 10 shallow GrCs present. Close SCs share some input from the same GrCs, but never from a completely identical set.

*4 excitatory and 24 inhibitory inputs*

**S2AAB:** As S1AA in which 6 close SCs (close meaning that they share some GrCs input) receive inhibitory input from 6 close BCs in B1AA, see description below.

*4 excitatory and 30 inhibitory inputs (6 of which are from BCs)*

**S3AABZ:** As S2AAB but the SCs inhibit the BCs as well, in the same manner. Identical to B3AASZ, see below.

*4 excitatory and 30 inhibitory inputs (6 of which are from BCs)*

**S4CL:** As S1AA but five close SCs have synapse weight 2E-9 between each other. The membrane potential of one of these cells is of interest.

*4 excitatory and* 24 *inhibitory inputs (four of which have weight 2E-9).*

## BC simulation

Receives only deep GrC input.
Synapse weight inhibitory: 3E-9.
Synapse weight excitatory: 3E-9.

**B1AA:** Network of 25 BCs, every BC inhibits all other BCs once. One BC receives input from 4 deep GrCs, totally 10 deep GrCs present. Close BCs share some input from the same GrCs, but never from a completely identical set.

*4 excitatory and 24 inhibitory inputs.*

**B2AAS:** As B1AA but close BCs receive inhibitory input from 6 close SCs in S1AA.

*4 excitatory and 30 inhibitory inputs (6 of which are from SCs).*

**B3AASZ:** As B2AAS but the BCs inhibit the SCs as well, in the same manner. This is the same network as S3AABZ.

*4 excitatory and 30 inhibitory inputs (6 of which are from SCs).*

**B4CL:** As B1AA but five close BCs have synapse weight 6E-9 between each other. The membrane potential of one of these cells is of interest.

*4 excitatory and emph24 inhibitory inputs (four of which have weight 6E-9).*

# SIMULATION 2

## SC simulation

Receives both shallow and deep GrC input, two from each.
Synapse weight inhibitory: 1E-9.
Synapse weight excitatory: 1E-9.

**S1AAsd:** Network of 25 SCs, every SC inhibits all other SCs once. One SC receives input from 2 shallow GrCs and 2 deep GrCs, totally 10 GrCs present (5 of each). Close SCs share some input from the same GrCs, but never from a completely identical set.

*4 excitatory and 24 inhibitory inputs.*

**S2AABsd:** As S1AAsd but 6 close SCs receive inhibitory input from 6 close BCs in B1AAsd, see description below.

*4 excitatory and 30 inhibitory inputs (6 of which are from BCs).*

**S3AABZsd:** As S2AABsd but the SCs inhibit the BCs as well, in the same manner. This is the same network as B3AASZsd. The 25 SCs and 25 BCs share the same deep and shallow GrCs for excitatory input, 10 GrCs in total, five of each.

*4 excitatory and 30 inhibitory inputs (6 of which are from BCs).*

**S4CLsd:** As S1AAsd but five close SCs have synapse weight 2E-9 between each other. The membrane potential of one of these cells is of interest.

*4 excitatory and 24 inhibitory inputs (four of which have weight 2E-9).*

## BC simulation

Receives both shallow and deep GrC input, two from each.
Synapse weight inhibitory: 3E-9.
Synapse weight excitatory: 3E-9.

**B1AAsd:** Network of 25 BCs, every BC inhibits all other BCs once. One BC receives input from 2 shallow GrCs and 2 deep GrCs, totally 10 GrCs present (5 of each). Close BCs share some input from the same GrCs, but never from a completely identical set.

*4 excitatory and 24 inhibitory inputs.*

**B2AASsd:** As B1AAsd but close BCs receive inhibitory input from 6 close SCs in S1AAsd.

*4 excitatory and 30 inhibitory inputs (6 of which are from SCs).*

**B3AASZsd:** As B2AASsd but the BCs inhibit the SCs as well, in the same manner. This is the same network as S3AABZsd. The 25 SCs and 25 BCs share the same

deep and shallow GrCs for excitatory input, 10 GrCs in total, five of each.

*4 excitatory and 30 inhibitory inputs (6 of which are from SCs).*

**B4CLsd:** As S1AAsd but five close BCs have synapse weight 6E-9 between each other. The membrane potential of one of these cells is of interest.

*4 excitatory and emph/24 inhibitory inputs (four of which have weight 6E-9).*

### Conclusions from SIMULATION 1 and 2:

SIMULATION 1 and 2 treats the two possible configurations between the MLIs and the GrCs. The first configuration, used in SIMULATION 1, is when the SCs only receive input from shallowly located GrCs while the BCs only receive input from deeply located GrCs. The second configurations is when the input to the SCs and the BCs is mixed between the shallowly and deeply located GrCs. The second configurations is used in SIMULATION 2 where the SCs and BCs receive half of their GrC-input from shallowly located GrCs and the other half from deeply located GrCs.

S1AAds and B1AAds show more realistic behavior than S1AA and B1AA, evaluated through visual comparison of their membrane potential, their variance and auto covariance. The remaining networks in SIMULATION 2 do not show realistic behavior which leads to the conclusion that the connections drawn are not valid. Therefore a new connectivity pattern is used in SIMULATION 3 below. The new connectivity pattern is called the star shape connection, see Fig. 2 in *Appendix B*.

## SIMULATION 3

### SC simulation

Receives both shallow and deep GrC input, two from each.

Synapse weight inhibitory: see network-description below.

Synapse weight excitatory: 1E-9.

**S1star:** Network of 25 SCs, groups of five, inhibits each other through the star shape connection, see Fig. 2 in *Appendix B*. One SC receives input from 2 shallow GrCs and 2 deep GrCs, totally 10 GrCs present (5 of each). Close SCs share some input from the same GrCs, but never from a completely identical set.
Two different weight sets for the inhibitory synapses:
1. 5E-9
2. 10E-9

*4 excitatory and 5 inhibitory inputs (synapse weight 5E-9 or 10E-9).*

**S2starB:** As S1star but 5 close SCs receive inhibitory input from 5 close BCs in B1star, see description below. Synapse weight BC to SC is 1E- 9.
Two different weight sets for the inhibitory synapses:

1. Among stellate: 5E-9, among basket 15E-9.
2. Among stellate: 10E-9, among basket 30E-9.

*4 excitatory and 10 inhibitory inputs (5 of which are from BCs, see specific weights above).*

**S3starBZ:** As S2starB weight set 2 but the SCs inhibit the BCs as well, in the same manner. This is the same network as B3starSZ. Synapse weight SC to BC is 3E- 9.

*4 excitatory and 10 inhibitory inputs (5 of which are from BCs, see specific weights above).*

**S4starBZrand:** As S3starBZ but the inhibitory synapses, BC to SC and SC to BC, are distributed randomly, five to each.

*4 excitatory and 10 inhibitory inputs (5 of which are from BCs, see specific weights above).*

## BC simulation

Receives both shallow and deep GrC input, two from each.

Synapse weight inhibitory: see network-description below.

Synapse weight excitatory: 3E-9

**B1star:** Network of 25 BCs, groups of five, inhibits each other through the star shape connection. One BC receives input from 2 shallow GrCs and 2 deep GrCs, totally 10 GrCs present (5 of each). Close BCs share some input from the same GrCs, but never from a completely identical set.
Two different weight sets for the inhibitory synapses:
1. 15E-9
2. 30E-9

*4 excitatory and 5 inhibitory inputs (synapse weight 15E-9 or 30E-9).*

**B2starS:** As B1star but 5 close BCs receive inhibitory input from 5 close SCs in S1star. Synapse weight SC to BC is 3E-9.
Two different weight sets for the inhibitory synapses:
3. Among stellate: 5E-9, among basket 15E-9.
4. Among stellate: 10E-9, among basket 30E-9.

*4 excitatory and 10 inhibitory inputs (5 of which are from SCs, see specific weights above).*

**B2starSrand:** As B2starS weight set 4 but the inhibitory synapses from SCs to BCs are randomly distributed, 5 to each BC, with synapse weight 3E-9.

*4 excitatory and 10 inhibitory inputs (5 of which are from SCs, see specific weight above).*

**B2NoStarS:** Network of 25 BCs, groups of five, no inhibition among them. One BC receives input from 2 shallow GrCs and 2 deep GrCs, totally 10 GrCs present (5 of each). Close BCs share some input from the same GrCs, but never from a completely identical set. Each group of BCs receives inhibitory synapses from each group of SCs in network S1star weight set 1 and 2. Synapse weight from SC to BC is 30E-9.
Two different weight sets for the inhibitory synapses among the SCs:
1. 5E-9
2. 10E-9

*4 excitatory and 5 inhibitory inputs (all of which are from SCs, see specific weights above).*

**B3starSZ:** As B2starS weight set 2 but the BCs inhibit the SCs as well, in the same manner. This is the same network as S3starBZ. Synapse weight BC to SC is 1E- 9.

*4 excitatory and 10 inhibitory inputs (5 of which are from SCs, see specific weights above).*

**B4starSZrand:** Same network as B3starSZ but the inhibitory synapses, BC to SC and SC to BC, are distributed randomly.

*4 excitatory and 10 inhibitory inputs (5 of which are from SCs, see specific weights above).*

### Conclusions from SIMULATION 3:

Network configuration S1star together with B1star, both with weight set 1, and S1star together with B2NoStarS, both with weight set 2, are deemed realistic. This is done by visual comparison of the membrane potential, evaluation of the spectral density estimate, auto covariance and variance by comparison to the experimental data. The remaining networks are deemed non-realistic by the same evaluation process. In SIMULATION 4 below, the two network configurations mentioned are investigated further by increasing their synapse weights and injecting a bias current.

## SIMULATION 4

### SC simulation

Receives both shallow and deep GrC input, two from each.

Synapse weight inhibitory: changes for the different networks, see description below.

Synapse weight excitatory: 1E-9.

**S1star20:** As S1star in Simulation constellation 3 above, but inhibitory synapse weights are 20E-9.

*4 excitatory and 5 inhibitory inputs (synapse weight 20E-9).*

**S1star20Bias:** As S1star20 but all cells receive bias.
Two different bias currents:
1. 5pA.
2. 15pA.

*4 excitatory and 5 inhibitory inputs (synapse weight 20E-9) + bias current.*

### BC simulation

Receives both shallow and deep GrC input, two from each.

Synapse weight inhibitory: changes for the different networks, see description below.

Synapse weight excitatory: 3E-9.

**B1star60:** As B1star in Simulation constellation 3 above, but inhibitory synapse weights are 60E-9.

*4 excitatory and 5 inhibitory inputs (synapse weight 60E-9).*

**B1star260Bias:** As B1star60 but all cells receive bias current.
Two different bias currents:
1. 5pA.
2. 15pA.

*4 excitatory and 5 inhibitory inputs (synapse weight 60E-9) + bias current.*

### Conclusions from SIMULATION 4:

These alternations of the network configuartions did not improve their behavior.

## SIMULATION 5

When the spiking behavior of network configuration S1Star/B1Star and S1Star/B2NoStar from SIMULATION 3 is evaluated, it is not similar to in vivo behavior. Therefore, the spike-parameter-values are altered, based on the information given in Sec. 2.2, until realistic behavior is found. This results in that the synapse weights need to be altered as well.

The final spike-parameter-values are given in Tab. 6 below and the new synapse weights are described in the following paragraphs. See Fig. 2 and 3 in *Appendix B* for pictures of the two network configurations. They are, from now on, stated as SYS1 and SYS2.

Table 6: Values of the spike parameters

| Parameter | Values |
|---|---|
| ISI mean | [0,500,-58,0.49] |
| ISI std intensity | [0,1000,-58,-0.4] |

### SYS1: S1Star in combination with B1Star

**S1star:** Network of 25 SCs, groups of five, inhibits each other through the star shape connection, see Fig. 2 in *Appendix B*. One SC receives input from 2 shallow GrCs and 2 deep GrCs, totally 10 GrCs present (5 of each). Close SCs share some input from the same GrCs, but never from a completely identical set.
Weight for the inhibitory synapses SCs: 5E-9
Weight for the excitatory synapses from GrCs: 1E-10
*4 excitatory and 5 inhibitory inputs (synapse weight 5E-9 or 10E-9).*

**B1star:** Network of 25 BCs, groups of five, inhibits each other through the star shape connection. One BC receives input from 2 shallow GrCs and 2 deep GrCs, totally 10 GrCs present (5 of each). Close BCs share some input from the same GrCs, but never from a completely identical set.
Weight for the inhibitory synapses from BCs: 1.5E-8
Weight for the excitatory synapses from GrCs: 1E-9
*4 excitatory and 5 inhibitory inputs (synapse weight 15E-9 or 30E-9).*

### SYS2: S1Star in combination with B2NoStarS

**S1star:** Network of 25 SCs, groups of five, inhibits each other through the star shape connection, see figure 8.2 in Appendix B. One SC receives input from 2 shallow GrCs and 2 deep GrCs, totally 10 GrCs present (5 of each). Close SCs share some input from the same GrCs, but never from a completely identical set.
Weight for the inhibitory synapses SCs: 5E-9
Weight for the excitatory synapses from GrCs: 1E-10
*4 excitatory and 5 inhibitory inputs (synapse weight 5E-9 or 10E-9).*

**B2NoStarS:** Network of 25 BCs, groups of five, no inhibition among them. One BC receives input from 2 shallow GrCs and 2 deep GrCs, totally 10 GrCs present (5 of each). Close BCs share some input from the same GrCs, but never from a completely identical set. Each group of basket cells receives inhibitory synapses from each group of SCs in network S1star above.
Weight for the inhibitory synapses from SCs: 1E-8
Weight for the excitatory synapses from GrCs: 3.5E-9
*4 excitatory and 5 inhibitory inputs (all of which are from SCs, see specific weights above).*

## Part 2: Input/output analysis of final network configurations

In this second part of the simulations, network configurations SYS1 and SYS2 are evaluated upon their input/output behavior by different types of input-currents to the GrCs. The GrCs are now modeled by the Leaky Integrate and Fire model with the

Escape Rate model for their spike generation. The membrane and spike parameter-values of the GrCs are stated in Tab. 7 below and Tab 6 on the previous page, respectively.

The output of SYS1 and SYS2 is the membrane potential of a PC which receives an inhibitory synapse from each MLI present in the network configurations. It is modeled in the same manner as the GrCs with the membrane-parameter-values stated in Tab. 7 on the following page. There is no interest in the spiking behavior of the PC.

The synapse weight for the inhibitory synapses upon the PC is 1E-7, decided upon that the membrane potential of the PC should decrease about 2-5 mV when the MLI spiking activity rises from 7 Hz to 70 Hz. The remaining synapse-parameter-values used are the ones stated in Tab. 5 for the inhibitory synapse, except that E=-80 mV instead.

## Part 3: Input/output analysis of final network configurations with feedback loop

In this third part of the simulations, a feedback loop is added to both SYS1 and SYS2. The same type of input/output analysis done in the previous simulation-part is performed for the network configurations with feedback loop as well.

The inhibitory synapses of the MLIs are now drawn to a spike-to-current converter, which uses the PC membrane-parameter-values in the conversion, additional to the PC. The feedback loop leads the current of the converter through a lowpass filter with cut-off frequency 10 Hz, gain of 0.2 and delay of 10 ms in order to simulate the in-vivo-path of the information back to the GrCs. These values of the feedback transfer function are derived from [Jörntell & Ekerot 2006, Fig. 2]. The output of the network configurations is still the membrane potential of the PC modeled by the Leaky Integrate and Fire model as in Part 2 of the simulations.

Table 7: Values of the membrane parameters for the GrCs and the PC

| Parameter | GrC | PC |
|---|---|---|
| $\tau$ (ms) | 2 | 15 |
| $R_m$ (MΩ) | 500 | 5 |
| $C_m = \tau / R_m$ (F) | 4E-12 | 3E-9 |
| $g_L = 1/R_m$ (S) | 2E-9 | 2E-7 |
| $E$ (mV) | 65 | 70 |
| $V$ (mV) | 0.5 | 0.5 |
| $K$ | 8 | 8 |

# Appendix B

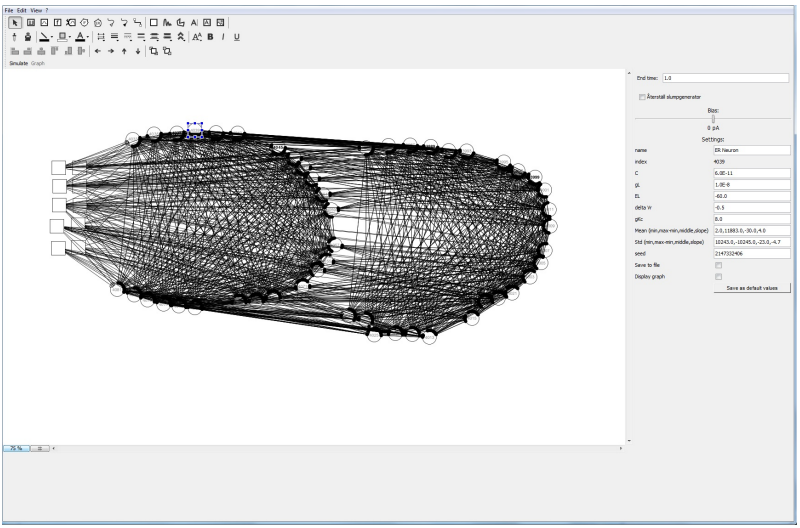

Figure 1: Picture of the simulation environment when simulating S3AABZ and B3AASZ in SIMULATION 1.

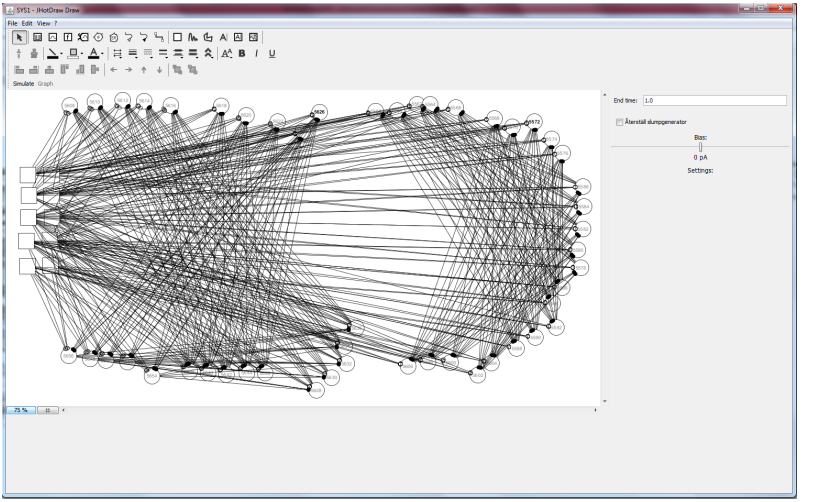

Figure 2: Picture of the simulation environment when simulating S1star and B1star in SIMULATION 2, 3 and 5.

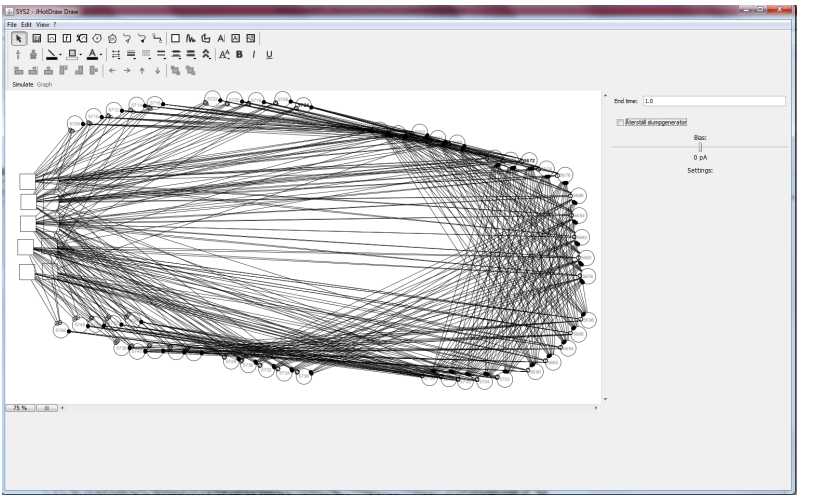

Figure 3: Picture of the simulation environment when simulating S1star and B2NoStarS in SIMULATION 2, 3 and 5.

# Bibliography

L. F. Abbott, Lapicque's introduction of the integrate-and-fire model neuron (1907), Brain Research Bulletin, 1999, 50:5-6, pp. 303 – 304.

T. Abrahamsson, L. Cathala, K. Matsui, R. Shigemoto and D. A. DiGregorio, Thin Dendrites of Cerebellar Interneurons Confer Sublinear Synaptic Integration and a Gradient of Short-Term Plasticity, Neuron, 2012, Volume 73, Issue 6, pp. 1159-1172.

F. Bengtsson and H. Jörntell, Sensory transmission in cerebellar granule cells relies on similarly coded mossy fiber inputs. Proc. of the National Academy of Sciences, 2009, 106:7, pp. 2389–2394.

J. Bergh, F. Ekstedt and M. Lindberg, Wavelets, Studentlitteratur, Lund, Sweden, 1999.

F. Briatore, A. Patrizi, L. Viltono, M. Sassoè-Pognetto and P. Wulff, Quantitative Organization of GABAergic Synapses in the Molecular Layer of the Mouse Cerebellar Cortex. PLoS ONE, 2010, 5(8): e12119.

E. D'Angelo, The critical role of golgi cells in regulating spatio-temporal integration and plasticity at the cerebellum input stage. Frontiers in Neuroscience, 2008, Volume 5:0, p. 5.

J. Dürango, Analysis and simulation of cerebellar circuitry. Master's Thesis ISRN TFRT- -5860. Department of Automatic Control, Lund University, Sweden, 2010.

C. F. Ekerot and H. Jörntell, Parallel fibre receptive fields of Purkinje cells and interneurons are climbing fibre-specific, Eur J Neurosci , 2001, 13: p. 1303-1310.

A. Ekholm and J. Hyvärinen, A pseudo-markov model for series of neuronal spike events, Biophysical Journal, 1970, 10:8, pp. 773 – 796.

R. F. Engle and C. W. J. Granger, Co-Integration and Error Correction: Representation, Estimation, and Testing. Econometrica, 1987, Vol. 55, No. 2. (Mar., 1987), pp. 251-276.

F. Gustavsson, L. Ljung and M. Millnert, Signal Processing, Studentlitteratur, Lund, Sweden, 2010.

B. Hille, Ion Channels of Excitable Membranes, 3rd edition, Sinauer Associates, Sunderland, MA, USA, 2001.

M. Ito, Control of mental activities by internal models in the cerebellum. Nature Reviews Neuroscience, 2008, 9:4, pp. 304–313.

A. Jakobsson, Time series analysis, Copyright Andreas Jakobsson, Lund, Sweden, 2011.

R. Johansson. System Modeling and Identification. Prentice Hall, Englewood Cliffs, New Jersey, 1993; (2nd ed.) KFS, Lund, Sweden, 2010. Appendix E: State Space Realization Theory.

I.T. Joliffe, Priciple component analysis, 2nd edition, Springer-Verlag, New York, USA, 2002.

H. Jörntell, F. Bengtsson, M. Schonewille, and C. I. De Zeeuw, Cerebellar molecular layer interneurons - computational properties and roles in learning, Trends in Neurosciences, 2010, 33:11, pp. 524 – 532.

H. Jörntell and C. Ekerot, Properties of somatosensory synaptic integration in cerebellar granule cells in vivo, The Journal of Neuroscience, 2006, 26:45, pp. 11786–11797.

H. Jörntell and C.-F. Ekerot, Receptive field plasticity profoundly alters the cutaneous parallel fiber synaptic input to cerebellar interneurons in vivo, The Journal of Neuroscience, 2003, 23:29, pp. 9620–9631.

H. Jörntell and C. F. Ekerot, Reciprocal bi-directional plasticity of parallel fiber receptive fields in cerebellar Purkinje cells and their afferent interneurons, Neuron, 2002, 34, p. 797-806.

C. Koch and I. Segev, Eds., Methods in Neuronal Modeling: From Ions to

Networks, 2nd edition. MIT Press, Cambridge, MA, USA, 1998.

MATLAB (2012): R2012b, The MathWorks Inc., Natick, MA.

S. L. Palay. and V. Shan-Palay, Cerebellar cortex: cytology and organization, Springer, Berlin, Germany, 1974.

B. Pesaran, Spectral Analysis for Neural Signals In: Neural Signal Processing: Quantitative Analysis of Neural Activity, 2008 (Mitra P, ed) pp. [1-12]. Washington, DC: Society for Neuroscience.

D. Purves, G. J. Augustine, D. Fitzpatrick, W. C. Hall, A.-S. LaMantia, J. O. McNamara, and S. M. Williams, Neuro Science, 3rd edition. Sinauer Associates, Sunderland, MA, USA, 2004.

T. J. H. Ruigrok, R. A. Hensbroek and J. I. Simpson, Spontaneous Activity Signatures of Morphologically Identified Interneurons in the Vestibulocerebellum, The Journal of Neuroscience, 12 January 2011, 31(2): pp. 712-724.

A. Spanne, Function of cerebellar microcircuitry within a closed-loop system during control and adaption. Master's Thesis ISRN TFRT- -5877, Department of Automatic Control, Lund University, Sweden, 2011.